Figure S1. Biochemical characterization of p53 monomers. (A) P53 monomers from enriched nuclear fractions migrated at 50 kDa according to SDS-PAGE and western blots. IB: immunoblot; primary antibodies were against the NTD of p53. **(B)** EM image of p53 monomers. Scale bar is 50 nm. **(C)** Class averages of p53 monomers, box size is 10 nm. Adapted from Solares et al, 2020[16].
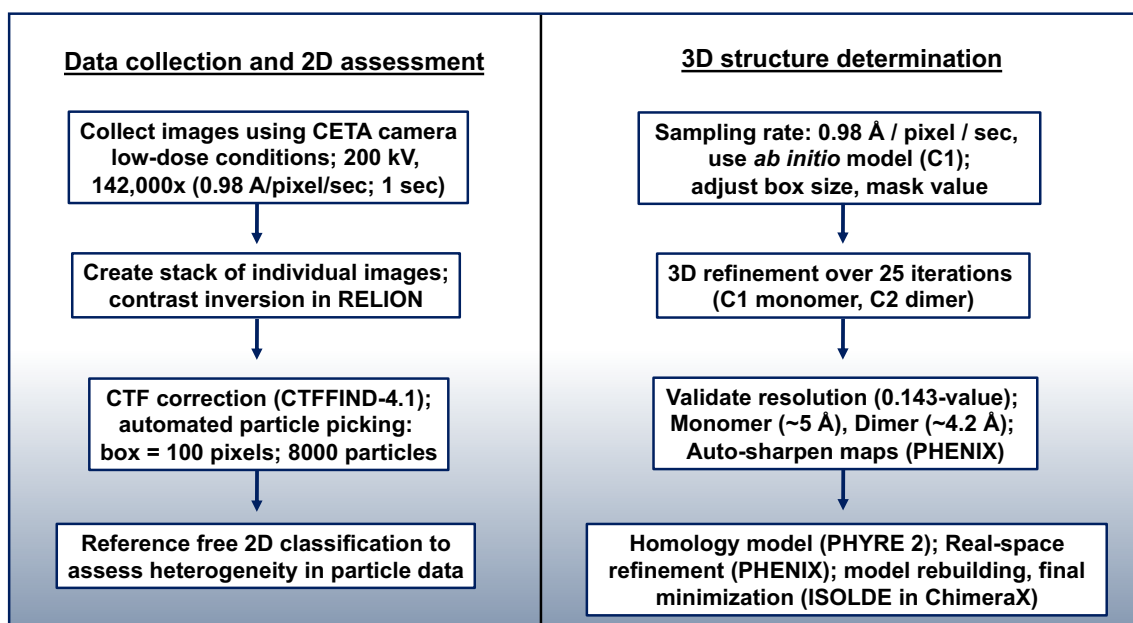
Figure S2. Workflow of image processing procedures. Images were collected using a CETA camera integrated into an F200C TEM operating in bright-field mode at 200 kV under low-dose conditions (~5 electron /Å^2/sec). The nominal magnification was 142,000x with a final sampling of 0.98 Å/pixel /sec at the specimen level for 1 second exposures. Images were processed in the RELION software package[29] and included CTF correction with automated particle picking using a box size of 100 pixels. 8000 total particles were selected for the p53 monomer and dimer structures. Reference-free classification procedures were performed using all particles that were subsequently employed for 3D refinement procedures. For 3D refinement, *ab initio* models were produced in RELION using C1 symmetry. Refinement cycles included 25 iterations to yield EM maps for each structure. C2 symmetry was used during refinement for the p53 dimer and C1 symmetry was used for the p53 monomer. The structural resolution was determined by comparing half-maps at the 0.143 value along with comparison to theoretical models, Cref (0.5) criteria. The p53 monomer resolution was ~5 Å and the p53 dimer resolution was ~4.2 Å. EM maps were imported into the PHENIX software package[30] and auto-sharpened at the resolution determined in RELION. A homology model for p53 was produced in PHYRE 2 and imported into PHENIX. Rigid-body refinement was performed using standard procedures. The output model was evaluated and rebuilt into the p53 monomer map using molecular dynamics-flexible fitting (MD-FF) procedures in the ISOLDE program[31] implemented in ChimeraX[33]. Final statistics for the p53 structure were evaluated using the Molprobity program[49] and are given in Table 1.
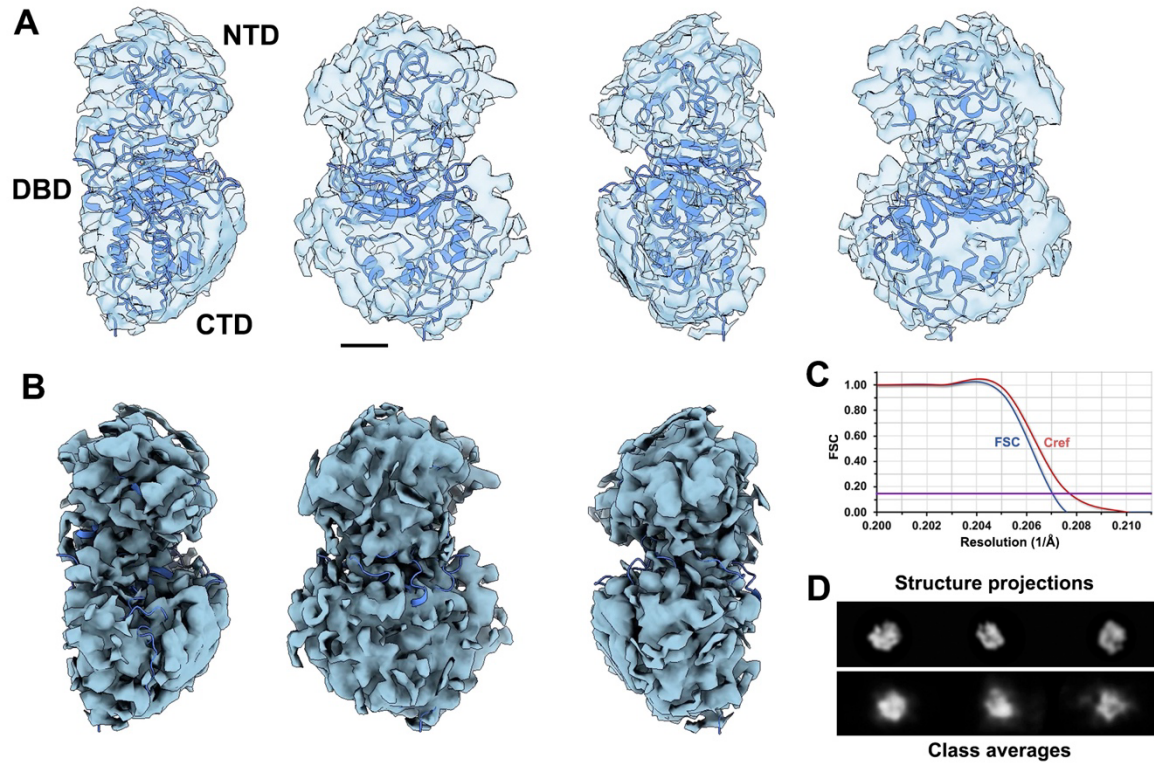
Figure S3. Cryo-EM structure of the p53 monomer (A) EM structure of the p53 monomer shown in different rotational views with transparent and solid rendering **(B)**. The structure was interpreted using an initial model that was fit into the map and subjected to rebuilding and refinement using the PHENIX and ISOLDE software packages. Scale bar is 5 Å. **(C)** The FSC curve and Cref (0.5) evaluation indicate a resolution of ~5 Å at the 0.143 value (purple line). **(D)** Comparison between structural projections of the p53 monomer (top row) and class averages (bottom row).

Movie S1. Rotational views of the p53 monomer. The EM map and model of full-length p53 (blue) shown in different rotational views about the y-axis. The NTD is positioned at the top of the structure, the DBD is in the middle of the map, and the CTD is located within the lower portion of the density.

Movie S2. The p53 model with rotation. The full-length p53 model (blue) is shown in different rotational views about the y-axis using the same view as Movie S1. The NTD is positioned at the top of the structure, the DBD is in the middle of the model, while the CTD is located at the bottom of the structure.

Movie S3. Rotational views of the inactive p53 dimer. The EM map of the full-length p53 dimer is presented in different rotational views. Monomers that comprise the dimer structure are colored blue and green. Models of the p53 monomer structure were fit into each half of the dimer map. Additional unoccupied density at the dimer interface suggested minor structural changes to each monomer upon binding.

Movie S3. Additional views of the inactive p53 dimer model. The p53 dimer model is presented in different rotational views. Models are colored blue and green to distinguish the individual monomers that comprise the dimer structure. The "crossed" architecture of the inactive structure may limit DNA binding to p53. Post-translational modifications (PTMs) to the p53 structure may limit dimer formation or relieve it as needed for on-demand repair events.

Movie S5. P53 inactive dimer release steps. Individual p53 models (blue and green) are released from their crossed, inactive state. Our data supports the notion that released proteins units undergo conformational changes to engage DNA (yellow).

Movie S6. P53 monomer assembly upon DNA. Models of p53 monomers (blue and green) can assemble upon double-stranded DNA (yellow) to form active dimers. This activation step may involve free, independent monomers or inactive dimers that are released from the crossed architecture in response to PTMs.

Movie S7. P53 reverse transition states. Models of the p53 dimer (blue and green) assembled on double-stranded DNA (yellow) during repair events. Following activation and repair p53 dimers are released from the DNA helix and reform the inactive conformation.